4776 *Chem. Mater.* **2010,** *22,* 4776–4782
DOI:10.1021/cm101314b

CHEMISTRY OF MATERIALS
Article

Efficient Light-Emitting Devices Based on Platinum-Complexes-Anchored Polyhedral Oligomeric Silsesquioxane Materials

Xiaohui Yang,[†] Jesse. D. Froehlich,[‡] Hyun Sik Chae,[‡] Brett T. Harding,[‡] Sheng Li,[‡] Amane Mochizuki,*[,‡] and Ghassan E. Jabbour*[,†,§]

[†]*School of Materials, Advanced Photovoltaic Center, Arizona State University, Tempe, Arizona, 85287-6006, and* [‡]*Nitto Denko Technical Corporation, 501 Via Del Monte, Oceanside, California 92058.* [§]*Current address: Solar and Alternative Energy Engineering Research Center, Physical Science and Engineering, KAUST, Thuwal, Saudi Arabia.*

Received May 10, 2010. Revised Manuscript Received June 25, 2010

The synthesis, photophysical, and electrochemical characterization of macromolecules, consisting of an emissive platinum complex and carbazole moieties covalently attached to a polyhedral oligomeric silsesquioxane (POSS) core, is reported. Organic light-emitting devices based on these POSS materials exhibit a peak external quantum efficiency of ca. 8%, which is significantly higher than that of the analogous devices with a physical blend of the platinum complexes and a polymer matrix, and they represent noticeable improvement in the device efficiency of solution-processable phosphorescent excimer devices. Furthermore, the ratio of monomer and excimer/aggregate electroluminescent emission intensity, as well as the device efficiency, increases as the platinum complex moiety presence on the POSS macromolecules decreases.

Introduction

Organic light-emitting diodes (OLEDs) remain excellent candidates for applications in next-generation flat-panel displays and solid lighting devices.[1,2] From materials perspective, OLEDs can be divided into two categories: (1) small molecules and (2) polymers. Small molecules are advantageous because they can be highly purified and vacuum-deposited in multilayer stacks, which are both important properties for display lifetime and efficiency. However, the material consumption and production cost of vacuum deposition techniques are relatively high. Moreover, fabrication of large-size full-color high- resolution OLED displays based on small molecules is formidable. Although polymers are generally of lower purity than small molecules and subject to batch-to-batch variation, they can be deposited via inkjet-printing[3] on larger substrates, making the fabrication of larger displays at much lower cost a possibility. Polyhedral oligomeric silsesquioxane (POSS) macromolecules bearing the carrier-transporting moieties or chromophores provide the advantages of both small-molecule and polymer light-emitting materials (i.e., high purity and solution processability including printing).[4,5] Encouraged by the advantages of POSS-based light-emitting materials, continued progress has been made on their use in OLED research. Sellinger et al.[5a] reported the synthesis of hole-transporting materials anchored POSS, which allowed for better device performance than the small-molecule analogues. Chen et al.[5b] reported the hydrosilylation of POSS with fluorophores and phosphors. Devices based on blending the iridium complex attached POSS with 4,4-*N*,*N*′-dicarbazole-biphenyl (CBP) and 1,3,5-tris(2-*N*-phenylbenzimidazolyl)benzene (TPBI) exhibited a turn-on voltage of 13 V, a maximum luminance efficiency of 3.99 cd A^{-1}, and maximum brightness of 1172 cd m^{-2}, with a peak emission of 524 nm. Froehlich et al.[5c] reported the functionalization of the POSS core with two different emitters in a controlled ratio, and they showed the possibility to realize multiple-wavelength emitting POSS. Single-layer light-emitting devices having such POSS materials in poly(*N*-vinylcarbazole) (PVK): 2-(4′-tert-butylphenyl)-5-(4′-diphenyl)-1,3,4-oxadiazole (PBD) matrix showed a turn-on voltage of ca. 10 V, a maximum external quantum efficiency (EQE) of 0.6%, and a luminance efficiency of 2.1 cd A^{-1} at 100 cd m^{-2}. Lo et al.[5d] reported the synthesis of POSS macromolecules with varying amounts of peripheral pyrene groups via Heck coupling reaction. Light-emitting devices with eight pyrene-substituted POSS as the emissive layer and TPBI as the hole/exciton-blocking layer exhibited an EQE value of 2.6% and a luminance efficiency of 8.3 cd A^{-1}. Very recently, we reported efficient monochromatic and white-emitting devices utilizing iridium-complex-functionalized POSS materials.[5e,f]

*Authors to whom correspondence should be addressed. E-mail addresses: Jabbour@asu.edu, Ghassan.jabbour@kaust.edu.sa (G.E.J.), amane.mochizuki@gg.nitto.co.jp (A.M.).

(1) Tang, C. W.; Vanslyke, S. A. *Appl. Phys. Lett.* **1987**, *51*, 913.
(2) Burroughes, J. H.; Bradley, D. D. C.; Brown, A. R.; Marks, R. N.; Mackay, K.; Friend, R. H.; Burn, P. L.; Holmes, A. B. *Nature* **1990**, *347*, 539.
(3) Singh, M.; Haverinen, H. M.; Dhagat, P.; Jabbour, G. E. *Adv. Mater.* **2010**, *22*, 673.
(4) (a) Laine, R. M. *J. Mater. Chem.* **2005**, *15*, 3725. (b) Chan, K. L.; Sonar, P.; Sellinger, A. *J. Mater. Chem.* **2009**, *19*, 9103.
(5) (a) Sellinger, A.; Tamaki, R.; Laine, R. M.; Ueno, K.; Tanabe, H.; Williams, E.; Jabbour, G. E. *Chem. Commun.* **2005**, *29*, 3700. (b) Chen, K. B.; Chang, Y. P.; Yang, S. H.; Hsu, C. S. *Thin Solid Films.* **2006**, *504*, 103. (c) Froehlich, J. D.; Young, R.; Nakamura, T.; Ohmori, Y.; Li, S.; Mochizuki, A.; Lauters, M.; Jabbour, G. E. *Chem. Mater.* **2007**, *19*, 4991. (d) Lo, M. Y.; Zhen, C. G.; Lauters, M.; Jabbour, G. E.; Sellinger, A. *J. Am. Chem. Soc.* **2007**, *129*, 5808. (e) Yang, X. H.; Froehlich, J. D.; Chae, H. S.; Li, S.; Mochizuki, A.; Jabbour, G. E. *Adv. Funct. Mater.* **2009**, *19*, 2623. (f) Singh, M.; Chae, H. S.; Froehlich, J. D.; Kondou, T.; Li, S.; Mochizuki, A.; Jabbour, G. E. *Soft. Mater.* **2009**, *5*, 3002.

Published on Web 07/21/2010

Square planar platinum complexes such as [2-(4′,6′-difluorophenyl)pyridinato-N,C$^{2'}$)] (2,4-pentanedionato) (FPt) display a combination of monomer and red-shifted excimer/aggregate emission in concentrated solution and solid films, which has been explored successfully in the fabrication of highly efficient white-emitting devices.[6] These so-called "phosphorescent excimer white-emitting devices" are of a simple device structure, utilizing only one emissive dopant to achieve white emission, and, as a result, can effectively minimize differential color aging encountered in white-emitting devices with multiple emissive dopants. Despite the advantages mentioned above, there are only few studies concerning solution-processable phosphorescent excimer devices. Furuta et al.[7a] reported the synthesis of multifunctional polymers containing various compositions of electron- and hole-transporting moieties as well as emitting platinum complexes via living polymerizations. Light-emitting devices based on the terpolymer showed an EQE value of 4.6% with Commission International de'l'É-clairage (CIE) coordinates of (0.33, 0.50). Norborene-derivatized platinum complex and 9,9-dialkyl-2,7-di-(carbazol-9-yl)fluorene monomers were synthesized and further copolymerized. It was observed that excimer/aggregate emission from platinum-complex moieties appeared in the electroluminescent (EL) spectra of light-emitting devices based on the copolymers.[7b] In this paper, we report the synthesis, photophysical, and electrochemical characteristics of POSS macromolecules bearing carbazole and platinum-complex moieties. The purpose of combining the carbazole and platinum-complex moieties onto the same POSS core is to effectively dilute the concentration of platinum complex in a single molecule, thereby adjusting the monomer and excimer/aggregate emission. The ratio of platinum complex to carbazole moiety incorporated onto POSS is shown to affect the monomer/excimer emission balance. In addition, light-emitting devices using such POSS macromolecules exhibit significantly higher efficiencies when compared to devices based on a physical blend of the platinum complexes and the polymer matrix. Furthermore, the ratio of monomer/excimer emission intensity in the EL spectrum and the device efficiency are shown to increase with decreased platinum-complex content of the POSS macromolecules.

Material Synthesis: General Information

All nonaqueous reactions were carried out under a dry, argon atmosphere, unless stated otherwise. Octakis(dimethylsilyloxy)POSS (**1**) was received from Aldrich. All other reagents and solvents were purchased from Aldrich or Gelest and were used as received, unless indicated otherwise. Column chromatography was performed using silica gel from ICN SiliTech (32-63ím). NMR data were collected using a JEOL ECL-400 system. Fluorescence measurements were performed on a Jobin Yvon Fluoromax 3 luminescence spectrometer. Ultraviolet−visible light (UV−vis) spectra were recorded on a Varian Cary 50 Scanspectrophotometer. Differential scanning calorimetry (DSC) measurements were performed on a Seiko Exstar 6000 DSC 6200 system. Thermogravimetric analysis (TGA) was performed on a Perkin−Elmer Pyris system. Cyclic voltammetry (CV) was performed using an Autolab type-II potentionsat/galvanostat model. Anhydrous DMF (Aldrich) was degassed and used as solvent under nitrogen atmosphere, while 0.1 M tetra(*n*-butyl)-ammonium hexafluorophosphate (NBu_4PF_6) was used as a supporting electrolyte. Silver wire was used as a reference electrode, and platinum wire was used as the counter electrode; glassy carbon was used as the working electrode. The redox potentials are based on the values relative to a ferrocene/ferrocenium (Cp_2Fe/Cp_2Fe^+) redox couple as an internal standard for calibration. CV data was recorded with a scan rate of 100 mV/s.

Scheme 1. Synthesis of the Platinum Complex[a]

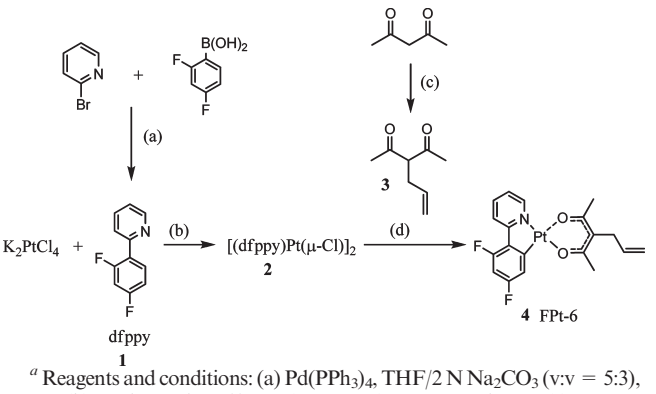

[a] Reagents and conditions: (a) $Pd(PPh_3)_4$, THF/2 N Na_2CO_3 (v:v = 5:3), 70 °C; (b) 2-ethoxyethanol/H_2O (v:v = 3:1), 80 °C, 16 h, N_2; (c) NaOH, MeOH, allylbromide; (d) Na_2CO_3, 2-ethoxyethanol, 100 °C, 16 h, N_2.

Experimental Procedure

2-(2,4-Difluorophenyl)pyridine (*dfppy*) ligand **1** was synthesized according to published literature.[8] Pt(II) μ-dichloro-bridged dimer, [(*dfppy*)Pt(μ-Cl)]$_2$ (**2**) and monomeric Pt(II) complexes (**4**) were prepared using an adapted synthetic procedure that has been detailed elsewhere.[9] Allyl-2,4-pentanedione (**3**) was synthesized in accordance with the literature.[10] (See Scheme 1.)

Synthesis of 1. 2-Bromopyridine (2.01 mL, 21.1 mmol), 2,4-difluorophenylboronic acid (4.00 g, 25.3 mmol), and tetrakis(triphenylphosphine)palladium(0) (0.732 g, 0.633 mmol) were added to a round-bottomed flask with a reflux condenser and dissolved in 10 mL of tetrahydrofuran (THF). After 6 mL of aqueous 2 N Na_2CO_3

(6) (a) Ma, B. W.; Djurovich, P. I.; Garon, S.; Alleyne, B.; Thompson, M. E. *Adv. Funct. Mater.* **2006**, *16*, 2438. (b) Williams, E. L.; Haavisto, K.; Li, J.; Jabbour, G. E. *Adv. Mater.* **2007**, *19*, 197. (c) Cocchi, M.; Kalinowski, J.; Virgili, D.; Fattori, V.; Develay, S.; Williams, J. A. G. *Appl. Phys. Lett.* **2007**, *90*, 163508. (d) Yang, X. H.; Wang, Z. X.; Madakuni, S.; Li, J.; Jabbour, G. E. *Adv. Mater.* **2008**, *20*, 2405. (e) Yang, X. H.; Wang, Z. X.; Madakuni, S.; Li, J.; Jabbour, G. E. *Appl. Phys. Lett.* **2008**, *93*, 193305.

(7) (a) Furuta, P. T.; Deng, L.; Garon, S.; Thompson, M. E.; Frechet, J. M. J. *J. Am. Chem. Soc.* **2004**, *126*, 15388. (b) Cho, J. Y.; Domercq, B.; Barlow, S.; Suponitsky, K. Y.; Li, J.; Timofeeva, T. V.; Jones, S. C.; Hayden, L. E.; Kimyonok, A.; South, C. R.; Weck, M.; Kippelen, B.; Marder, S. R. *Organometallics* **2007**, *26*, 4816.

(8) (a) You, Y. M.; Park, S. Y. *J. Am. Chem. Soc.* **2005**, *127*, 12438. (b) Lohse, O.; Thevenin, P.; Waldvogel, E. *Synlett*. **1999**, *1*, 45. (c) Xu, M. L.; Li, W. L.; An, Z. W.; Zhou, Q.; Wang, G. Y. *Appl. Organomet. Chem.* **2005**, *19*, 1225.

(9) (a) Brooks, J.; Babuyan, Y.; Lamansky, S.; Djurovich, P. I.; Tsyba, I.; Bau, R.; Thompson, M. E. *Inorg. Chem.* **2002**, *41*, 3055. (b) Cockburn, B. N.; Howe, D. V.; Keating, T.; Johnson, B. F. G; Lewis, J. *J. Chem. Soc. Dalton. Trans.* **1973**, *4*, 404.

(10) Davis, R. B.; Hurd, P. *J. Am. Chem. Soc.* **1955**, *77*, 3284.

was delivered, the reaction mixture was heated at 70 °C for 1 day. The cooled crude mixture was poured onto water and extracted with CH_2Cl_2 (50 mL × 3 times), then dried over anhydrous magnesium sulfate ($MgSO_4$). Finally silica column purification (*n*-hexane: EtOAc = 4:1) gave a transparent liquid (3.90 g, 97%) in quantitative yield. ^{1}H NMR ($CDCl_3$, 400 MHz): δ 6.89 (m, 1H), 7.1 (m, 1H), 7.28 (m, 1H), 7.75 (m, 2H), 8.00 (m, 1H), 8.71 (d, J = 3.5 Hz, 1H).

Synthesis of 2. K_2PtCl_4 (Aldrich) (3.08 g, 7.40 mmol) and 2.5 equivalent of *dfppy* (**1**) (3.55 g, 18.6 mmol) were mixed and dissolved in a 3:1 ratio of 2-ethoxyethanol and water. The resulting yellow mixture was heated to 80 °C for 16 h under a N_2 atmosphere. The cooled reaction mixture was then quenched with cold water, giving a pale yellow-greenish powder. The resulting powder was filtered off by a frit via vacuum filtration and dried in air and then under vacuum, giving a quantitative yield (4.43 g, 98%) of pale-yellow powder (**2**). **2** was used for the next reaction without further purification.

Synthesis of 3. Sodium hydroxide (NaOH) (4.5 g, 113 mmol) was dissolved in anhydrous MeOH. After cooling the mixture using an ice bath at 0 °C, acetylacetone (10 g, 99.8 mmol) was added while stirring for several minutes. Allyl bromide (10.4 mL, 123 mmol) was then added without cooling over a period of 10 min. The reaction mixture was refluxed for 2 h, then cooled and filtered to remove excess NaBr. Methanol (MeOH) and the excess allyl bromide were removed by distillation, collecting 6.72 g (48% yield) of yellow oil at 81−87 °C. ^{1}H NMR ($CDCl_3$, 400 MHz): δ 5.86−5.79 (m, 0.5 H), 5.72−5.63 (m, 0.5 H), 5.10−4.97 (m, 2H), 3.71 (t, J = 7.7 Hz, 0.4 H), 2.97 (m, 1H), 2.58 (app t, J = 8.04 Hz, 1H), 2.17 (s, 3H), 2.09 (s, 3H).

Synthesis of FPt-6. 2 (4.35 g, 5.17 mmol), 2.6 equiv of **3** (1.88 g, 13.4 mmol), and 10 equiv of sodium carbonate, Na_2CO_3 (5.48 g, 51.7 mmol) were dissolved in 2-ethoxyethanol and heated to 100 °C for 16 h under N_2 atmosphere. After the reaction mixture was cooled, it was filtered through white salt and evaporated under a reduced pressure. Dark yellow crude was extracted with EtOAc (100 mL), brine (50 mL), and water (100 mL × 3 times). The organic crude was then run through a silica-gel chromatography with 2:3 ratio of DCM and *n*-hexane. **4** was further purified by a recrystallization with dichloromethane (DCM):methanol, giving 1.25 g (23% yield) of a pale yellow-greenish powder. ^{1}H NMR ($CDCl_3$, 400 MHz); δ 8.89 (d, J = 5.88 Hz, 1H), 7.95 (d, J = 8.4 Hz, 1H), 7.82 (t, J = 7.32 Hz, 1H), 7.12−7.08 (m, 2H), 6.57 (dtd, J = 2.16, 2.60, and 9.64 Hz, 1H), 5.93−5.86 (m, 1H), 5.05−5.01 (m, 2H), 3.08 (m, 2H), 2.11 (s, 3H), 2.09 (s, 3H). MS (MALDI): Calcd for $C_{19}H_{17}F_2NO_2Pt$, 524.42; Found, 525. Anal. Calcd for $C_{19}H_{17}F_2NO_2Pt$: C, 43.52; H, 3.27; N, 2.67; Found: C, 43.58; H, 3.36; N, 2.70.

Host Synthesis. The carbazole host (**H1**) was synthesized by reacting 9H-carbazole with allyl bromide and NaOH in dimethyl sulfoxide (DMSO) at 60 °C for 3 h. (See step a in Scheme 2.) The crude product was purified by column chromatography using 1:4 DCM:hexane as the eluent to yield an off-white solid (73%). ^{1}H NMR (400 MHz $CDCl_3$) δ 8.14 (d, J = 7.7 Hz, 2H), 7.49 (t, J = 8.0 Hz, 2H), 7.40 (d, J = 8.0 Hz, 2H), 7.27 (t, J = 8.0 Hz, 2H), 6.05 − 5.96 (m, 1H), 5.18 (d, J = 10.3 Hz, 1H), 5.06 (d, J = 17.2 Hz, 1H). Anal. Calcd for $C_{15}H_{13}N$: C, 86.92; H, 6.32; N, 6.76; Found: C, 87.04; H, 6.41; N, 6.77.

The MCP analog host (**H2**) was synthesized in four steps at 38% overall yield. (See steps b−e in Scheme 2.) Each intermediate and the final product were purified by aqueous work-up (using either ethyl acetate or DCM as the organic portion), followed by a normal-phase silica column in 0%−20% ethyl acetate in hexane. To start, 3,5-dibromophenol (**1**) was protected with chloromethylmethyl ether in the presence of sodium hydride in anhydrous acetone at −78 °C. The 3,5-dibromobenzene-1-methoxymethyl ether (**2**), a light yellow oil, was isolated in 90.5% yield. **2** was subjected to amination by 9*H*-carbazole under typical Buchwald−Hartwig conditions ($Pd(OAc)_2$, $P(t\text{-}Bu)_3$, NaOtBu, dry toluene, 120 °C) and **3** was collected from the column as an airy white powder in 57% yield. **3** was deprotected using HCl in dimethyl formamide (DMF), and the free phenol (**4**) was isolated in 96% yield as an off-white solid. Finally, the alkene tether was added by stirring **4** with 6-chlorohex-1-ene in DMF in the presence of excess potassium hydroxide and sodium iodide for 16 h at 80 °C. The target material (**H2**) was isolated as an off-white solid in 78% yield. ^{1}H NMR (400 MHz $CDCl_3$) δ 8.155 (d, J = 7.7 Hz, 4H) 7.588 (d, J = 8.04 Hz, 4H) 7.454 (t, J = 7.3 Hz, 4H) 7.407 (t, J = 1.6 Hz, 1H) 7.314 (t, J = 7.34 Hz, 4H) 7.232 (d, J = 1.84 Hz, 2H) 5.839 (m, 1H) 5.052 (dd, J_L = 17.2 Hz, J_s = 1.48 Hz, 1H) 4.991 (d, J = 10.28 Hz, 1H) 4.081 (t, J = 6.6 Hz, 2H) 2.160 (q, J = 6.96 Hz, 2H) 1.885 (m, 2H) 1.620 (m, 2H). Anal. Calcd for $C_{36}H_{30}N_2O$: C, 85.34; H, 5.97; N, 5.53; Found: C, 85.66; H, 6.30; N, 5.65.

Scheme 2. Synthesis of the Carbazole Host (H1) and the MCP Analog Host (H2)[a]

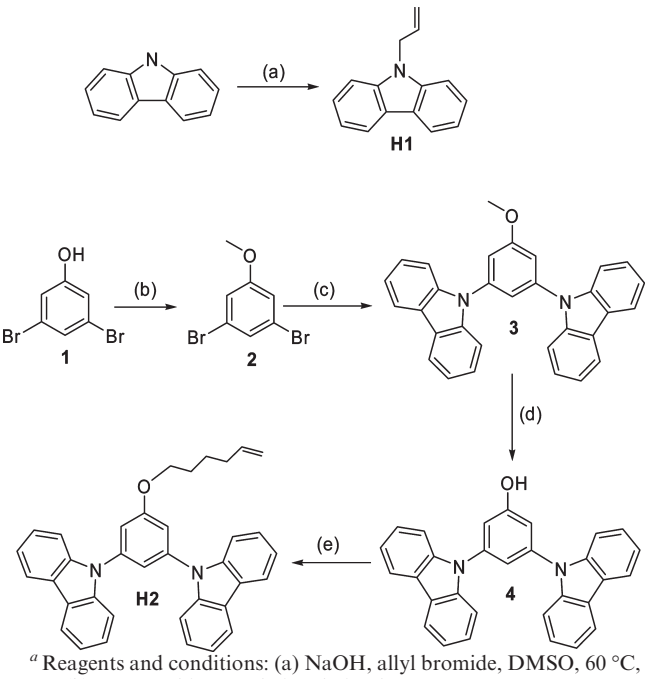

[a] Reagents and conditions: (a) NaOH, allyl bromide, DMSO, 60 °C, 73%; (b) NaH, chloromethylmethyl ether, acetone, −78 °C−RT, 91%; (c) carbazole, $Pd(OAc)_2$, $P(t\text{-}Bu)_3$, NaOtBu, toluene, 120 °C, 57%; (d) HCl, DMF, 45 °C; (e) 1-chlorohexene, KOH, NaI, DMF, 80 °C, 78%.

POSS Materials Synthesis. *General Reaction of POSS, FPt-6, and N-allylcarbazole.* To a solution of 868 mg (0.853 mmol) of octakis(dimethylsilyloxy)POSS and 447 mg (0.853 mmol) of FPt-6 in 20 mL anhydrous toluene, 4 drops of a solution of platinum-(0)-1,3-divinyl-1,1,3,3-tetramethyldisiloxane (Pt(dvs)) (2 wt % Pt in xylene) were added. The reaction mixture was stirred at room temperature for 1 h and then 1.765 g (8.53 mmol) of **H1** was added and the reaction mixture was stirred for an additional 16 h. The reaction mixture was then precipitated out of cold methanol and filtered through a silica plug, using DCM as the eluent. The crude material was then subjected to purification by column chromatography, using 1:4 ethyl acetate:hexane to yield pure fractions of

$POSS(FPt)_1(CBZ)_7$ and $POSS(FPt)_2(CBZ)_6$, which were isolated separately.

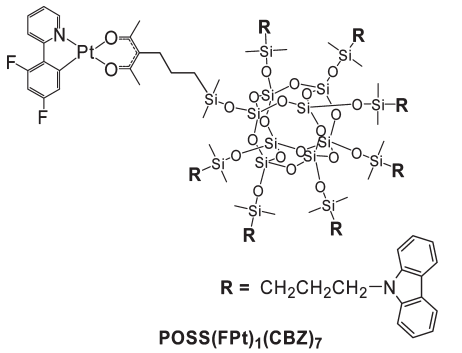

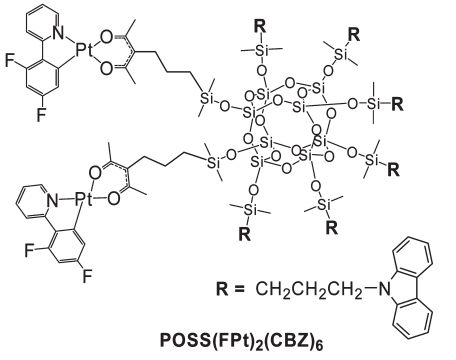

POSS(FPt-6)$_1$(CBZ)$_7$. ^{1}H NMR (400 MHz, $CDCl_3$): δ 8.82 (d, J = 5.1 Hz, 1H), 8.02 (d, J = 7.7 Hz, 14H), 7.85 (d, J = 8.4 Hz, 1H), 7.70 (t, J = 8.4 Hz, 1H), 7.36 (t, J = 7.7 Hz, 14H), 7.28−7.24 (m, 14H), 7.14 (t, J = 7.0 Hz, 14H), 7.10 (m, 1H), 6.93 (t, J = 6.2 Hz, 1H), 6.54 (t, J = 9.2 Hz, 1H), 4.13−4.05 (m, 14H), 2.24−2.20 (m, 2H), 2.05 (s, 3H), 2.04 (s, 3H), 1.80−1.75 (m, 14H), 1.45−1.39 (m, 2H), 0.58−0.53 (m, 16H), 0.006−(−0.03) (m, 48H). MS (MALDI): Calcd for $C_{140}H_{164}F_2N_8O_{22}PtSi_{16}$, 2991.8; Found, 2992.0.

POSS(FPt-6)$_2$(CBZ)$_6$. ^{1}H NMR (400 MHz, $CDCl_3$): δ 8.77 (d, J = 5.9 Hz, 2H), 8.02 (d, J = 7.7 Hz, 12H), 7.82−7.78 (m, 2H), 7.70−7.66 (m, 2H), 7.37−7.34 (m, 12H), 7.30−7.26 (m, 12H), 7.16−7.12 (m, 12H), 7.06−7.01 (m, 2H), 6.93−6.90 (m, 2H), 6.54−6.49 (m, 2H), 4.15−4.07 (m, 12H), 2.24−2.20 (m, 4H), 2.05−2.02 (m, 12H), 1.84−1.79 (m, 12H), 1.45−1.42 (m, 4H), 0.06−0.56 (m, 16H), 0.10−(−0.03) (m, 48H). MS (MALDI): Calcd for $C_{140}H_{164}F_2N_8O_{22}PtSi_{16}$, 3308.8; Found, 3311.7.

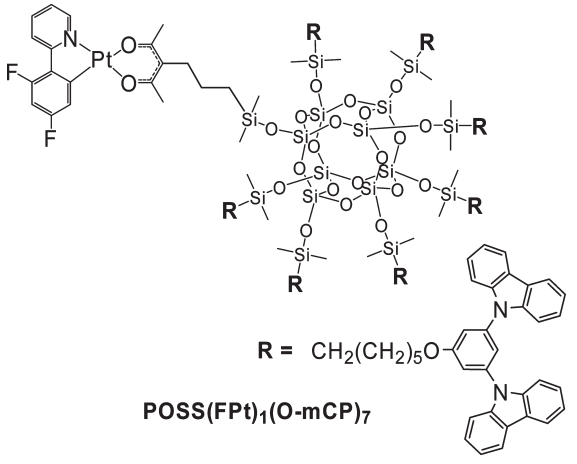

POSS(FPt-6)$_1$(O-mCP)$_7$. $POSS(FPt\text{-}6)_1(O\text{-}mCP)_7$ was synthesized under the same conditions as $POSS(FPt\text{-}6)_1(CBZ)_7$, except **H2** was used as the host moiety in place instead of **H1**.

^{1}H NMR (400 MHz, $CDCl_3$): δ 8.87−8.80 (m, 1H), 8.10−8.06 (m, 28H), 7.80−7.71 (m, 2H), 7.54−7.52 (m, 28H), 7.40−7.35 (m, 35H), 7.27−7.22 (m, 28H), 7.14 (s, 14H), 7.09 (m, 1H), 6.90−6.88 (m, 1H), 6.46−6.44 (m, 1H), 3.92−3.88 (m, 14H), 2.29−2.26 (m, 2H), 2.06−2.05 (m, 6H), 1.73−1.70 (m, 14H), 1.38−1.30 (m, 44H), 0.62−0.53 (m, 16H), 0.08−0.05 (m, 48H). MS (MALDI): Calcd for $C_{140}H_{164}F_2N_8O_{22}PtSi_{16}$, 5086.7; Found, 5093.0 (also found 5074.4 and 5109.7, corresponding to $POSS(mCP)_8$ and $POSS(FPt\text{-}6)_2(mCP)_6$, respectively).

OLED Fabrication. Poly[3,4-ethylenedioxythiophene] doped with poly[styrenesulfonate] (PEDOT:PSS) (CLEVIOS P VP AI 4083) was spin-coated onto precleaned and O_2-plasma-treated indium tin oxide (ITO) substrates, yielding layers ca. 80 nm thick. PEDOT:PSS layers were heated at 180 °C for 10 min to remove residual water. Blends of FPt-6-containing POSS + 30% 1,3-bis[(4-tert-butylphenyl)-1,3,4-oxidazolyl]phenylene (OXD-7) in chloroform solution was spin-coated on top of the PEDOT:PSS layers, yielding films ca. 70 nm thick. The samples were then dried at 80 °C for 30 min. For some devices, a TPBI hole/exciton-blocking layer was deposited via thermal evaporation at a rate of 0.06 nm s^{-1}. A cathode consisting of an ultrathin CsF interfacial layer with a nominal thickness of 1.5 nm and an Al layer ca. 100 nm thick was deposited by thermal evaporation. The deposition rates for CsF and Al were 0.005 and 0.2 nm s^{-1}, respectively. Individual devices have an area of 0.14 cm^2. All device fabrication, except spin-coating of the PEDOT:PSS layer, was carried out in a nitrogen-filled glovebox (Vac-atmosphere). Spectra were measured with an Ocean Optics Model HR4000 spectrometer; current-voltage ($I-V$) measurements were obtained using a Keithley Model 2400 SourceMeter, and light output was measured using a Newport Model 2832-C power meter and a Newport Model 818 UV detector. Unless specified otherwise, all device measurements were performed inside a nitrogen-filled glovebox.

Results and Discussion

A phosphorescent platinum complex capable of both monomer and excimer/aggregate emission and carbazole material are covalently attached to the same POSS core. This approach is used to eliminate the need to mix the emitter into a polymer or small molecule host, thus reducing aggregation of the emitter molecules. The carbazole moieties are chosen because they have good hole-transporting properties and have been shown to be good hosts for platinum-based emitters.[6] A terminal alkene is first attached to the platinum complex and carbazole moieties to react with POSS under hydrosilylation conditions. The platinum complex/carbazole-functionalized POSS is synthesized in a stepwise fashion by sequentially reacting the FPt-6 with POSS in a 1:1 ratio, followed by reaction with excess carbazole moieties. The resulting reaction mixture can then be separated chromatographically, resulting in monodisperse POSS materials in the case of $POSS(FPt\text{-}6)_1(CBZ)_7$ and $POSS(FPt\text{-}6)_2(CBZ)_6$. However, $POSS(FPt\text{-}6)_1(O\text{-}mCP)_7$ is shown to contain other peaks in the mass spectrum, corresponding to $POSS(O\text{-}mCP)_8$ and $POSS(FPt\text{-}6)_2(O\text{-}mCP)_6$. These POSS materials are highly soluble in most organic solvents and have good film-forming characteristics.

The photophysical, electrochemical, and thermal properties of FPt-6-anchored POSS macromolecules are summarized in Table 1. The absorption of POSS macromolecules can be attributed to the absorption of metal-to-ligand charge-transfer (MLCT) states of FPt-6 units at ca. 340−350 nm[9a]

Table 1. Photophysical, Electrochemical, and Thermal Properties of FPt-Complexes-Anchored POSS Macromolecules

compound	Solution[a]		Solid Film[b]		
	λ_{max} [nm]	λ_{max} [nm][c]	λ_{max} [nm]	$T_{d5\%}$ [°C][d]	redox $E_{1/2}^{Red}$ [V][e]
POSS(FPt-6)$_1$(carbazole host)$_7$	265, 296, 348	353*, 366*, 464, 491	465, 498, 580	300	−2.33
POSS(FPt-6)$_2$(carbazole host)$_6$	265, 296, 347	351*, 366*, 464, 491	467, 501, 582	284	−2.33
POSS(FPt-6)$_1$(mCP)$_7$	294, 327, 340	345*, 360*, 465, 495	466, 498, 529, 580	308	−2.33

[a] Measured in dilute chloroform solution. [b] Drop-cast neat film. [c] Asterisk (*) indicates emission from carbazole moieties. The remaining values are the emission peaks of the FPt complex. [d] The temperature in N_2 atmosphere at which 5 wt % loss has occurred. [e] Measured in DMF solution; values versus potential of ferrocene/ferricenium couple.

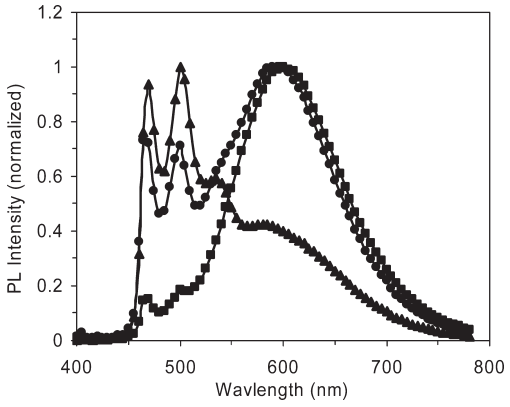

Figure 1. Photoluminescence spectra of (●) POSS(FPt-6)$_1$(CBZ)$_7$, (■) POSS(FPt-6)$_2$(CBZ)$_6$, and (▲) POSS(FPt-6)$_1$(O-mCP)$_7$ solid films.

and carbazole units, together with ligand-centered absorption of FPt-6 units at shorter wavelength. Emission from the FPt-6 and carbazole units can be observed in the photoluminescence spectra of POSS materials in diluted chloroform solution, whereas in the solid state, emission from carbazole units is significantly diminished, as a result of enhanced energy transfer to the FPt-6 units, as shown in Figure 1. When increasing the FPt-6 substitution on the POSS from **1** to **2** (as in POSS(FPt-6)$_1$(CBZ)$_7$ versus POSS(FPt-6)$_2$(CBZ)$_6$)), it can be seen that the monomer emission from FPt-6 moieties (with emission peaks at 465 and 500 nm) is dramatically reduced, with respect to that of the excimer/aggregate emission (with emission peak at 580 nm). This is due to the effective increase in the FPt-6 concentration in the material, which favors emission from the excimer/aggregate states. Increasing the amount of the carbazole moieties, as in POSS(FPt-6)$_1$(CBZ)$_7$ versus POSS(FPt-6)$_1$(O-mCP)$_7$, results in an increase in the monomer emission in the solid state (Figure 1). In an electrochemistry study, all three POSS macromolecules show a single irreverisble oxidation wave; meanwhile, a common reversible reduction wave at −2.33 V can be observed (see Table 1). The electrochemical properties of FPt-6 anchored POSS macromolecules are the same as that of FPt-6.[9a]

The POSS macromolecules show improved thermal stability, compared to the parent platinum complex (e.g., for POSS(FPt-6)$_1$(O-mCP)7, $T_d \approx 300$ °C, which is higher than that of FPt-6 ($T_d \approx 255$ °C)).

Organic Light-Emitting Devices. To investigate the EL properties of POSS macromolecules, light-emitting devices with two types of architectures have been made and compared: (I) ITO/PEDOT:PSS/70 nm POSS(FPt-6)$_1$(O-mCP)$_7$ + 30% OXD-7 (by weight)/CsF/Al; (II) ITO/PEDOT:PSS/70 nm POSS(FPt-6)$_1$(O-mCP)$_7$ + 30% OXD-7 (by weight)/30 nm TPBI/CsF/Al. The design of device structure follows a previous study on solution-processable electrophosphorescent devices.[11] Comparison of devices with OXD-7 (type I) and without OXD-7 (i.e., ITO/PEDOT:PSS/70 nm POSS-(FPt-6)$_1$(O-mCP)$_7$/CsF/Al (not shown)) indicates that the addition of electron-transporting OXD-7 reduces the turn-on voltage, enhances the device luminance, and improves the device efficiency by almost 1 order of magnitude. This is attributed to improvement of electron injection/transport and reduction of cathode quenching as generally observed in solution-processable electrophosphorescent devices.[11] In addition, the significant improvement in device performance upon addition of OXD-7 implies that possible electron transport among FPt-6 moieties is rather weak. Figure 2 shows the characteristics of type I and type II devices. Detailed properties of devices are summarized in Table 2. As shown in Figure 2a, type II devices exhibit a higher drive voltage at a given current density, compared to that for type I devices, which can be attributed to an overall larger layer thickness in type II devices and the hole-blocking effect of the TPBI layer. Meanwhile, incorporation of a TPBI layer enhances EQE, because of improved balance of carrier injection and transport (Figure 2b). The EL spectra of devices (see Figure 2c), which show the high-energy structured monomer emission and broad excimer/aggregate emission, are not significantly affected by the insertion of the TPBI layer. In fact, incorporation of the TPBI layer improves the efficiency and does not affect the EL spectra of any of the POSS-based devices presented in this study. Therefore, the type II device structure is adopted to characterize the EL properties of POSS macromolecules.

Compared to the PVK control devices, where 12% FPt is embedded in PVK + 30% OXD-7 host, the current density−bias voltage characteristics of POSS-macromolecules-based devices (Figure 3a) shift to higher drive voltages, such that $V_{POSS(FPt\text{-}6)1(O\text{-}mCP)_7} < V_{POSS(FPt\text{-}6)1(CBZ)_7} < V_{POSS(FPt\text{-}6)2(CBZ)_6}$, indicating that carbazole moieties in the POSS materials

(11) (a) Vaeth, K. M.; Tang, C. W. *J. Appl. Phys.* **2002**, *92*, 3447. (b) Yang, X. H.; Neher, D.; Hertel, D.; Daeubler, T. K. *Adv. Mater.* **2004**, *16*, 161. (c) Yang, X. H.; Neher, D. *Appl. Phys. Lett.* **2004**, *84*, 2476. (d) Wu, F. I.; Luo, L. Y.; Diau, W. G.; Cheng, C. H.; Duan, J. P.; Lee, G. H. *J. Mater. Chem.* **2005**, *15*, 1035. (e) Wu, F. I.; Shih, P. I.; Tseng, Y. H.; Chen, G. Y.; Chien, C. H.; Tung, Y. L.; Chi, Y.; Jen, A. K. Y. *J. Phys. Chem. B* **2005**, *109*, 14000. (f) Wu, F. I.; Shih, P. I.; Shu, C. F.; Tung, Y. L.; Chi, Y. *Macromolecules* **2005**, *38*, 9028. (g) Yang, X. H.; Jaiser, F.; Klinger, S.; Neher, D. *Appl. Phys. Lett.* **2006**, *88*, 021107. (h) Yang, X. H.; Muller, C. D.; Neher, D.; Meerholz, K. *Adv. Mater.* **2006**, *18*, 948. (i) Yang, X. H.; Jaiser, F.; Stiller, B.; Neher, D.; Galbrecht, F.; Scherf, U. *Adv. Funct. Mater.* **2006**, *16*, 2156. (j) Zacharias, P.; Gather, M. C.; Rojahn, M.; Nuyken, O.; Meerholz, K. *Angew. Chem., Int. Ed.* **2007**, *46*, 4388. (k) Huang, F.; Niu, Y. H.; Zhang, Y.; Ka, J. W.; Liu, M. S.; Jen, A. K. Y. *Adv. Mater.* **2007**, *19*, 2010.

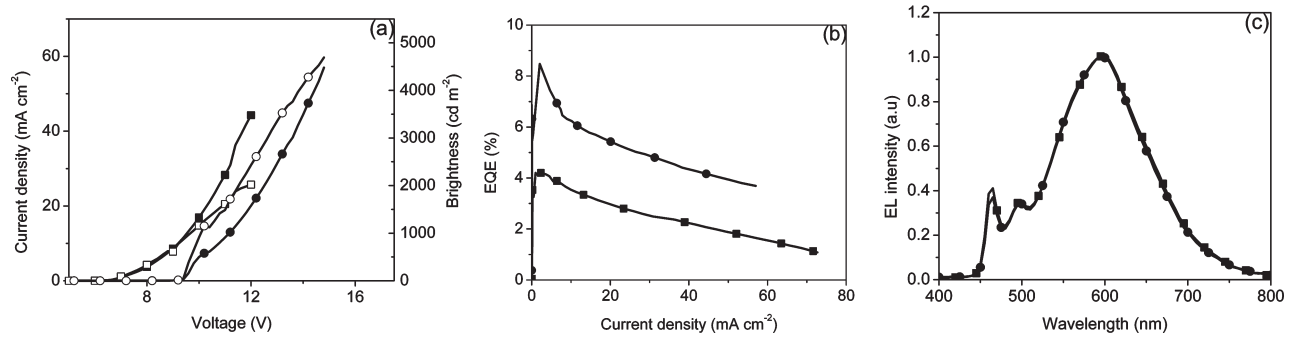

Figure 2. (a) Graph showing the properties of POSS(FPt-6)$_1$(O-mCP)$_7$ devices: (a) current density (solid symbols) and luminance (open symbols) versus bias voltage characteristics of POSS(FPt-6)$_1$(O-mCP)$_7$ devices with type I configurations (ITO/PEDOT:PSS/POSS(FPt-6)$_1$(O-mCP)$_7$ + 30% OXD-7/CsF/Al) or type II configurations (ITO/PEDOT:PSS/POSS(FPt-6)$_1$(O-mCP)$_7$ + 30% OXD-7/TPBI/CsF/Al). (b) Graph showing the external quantum efficiency−current density properties. (c) Graph showing the normalized electroluminescent (EL) spectra. [Throughout this figure, data for ITO/PEDOT:PSS/POSS(FPt-6)$_1$(O-mCP)$_7$ + 30% OXD-7/CsF/Al are denoted as squares) and data for ITO/PEDOT:PSS/POSS(FPt-6)$_1$(O-mCP)$_7$ + 30% OXD-7/TPBI/CsF/Al are denoted as circles.]

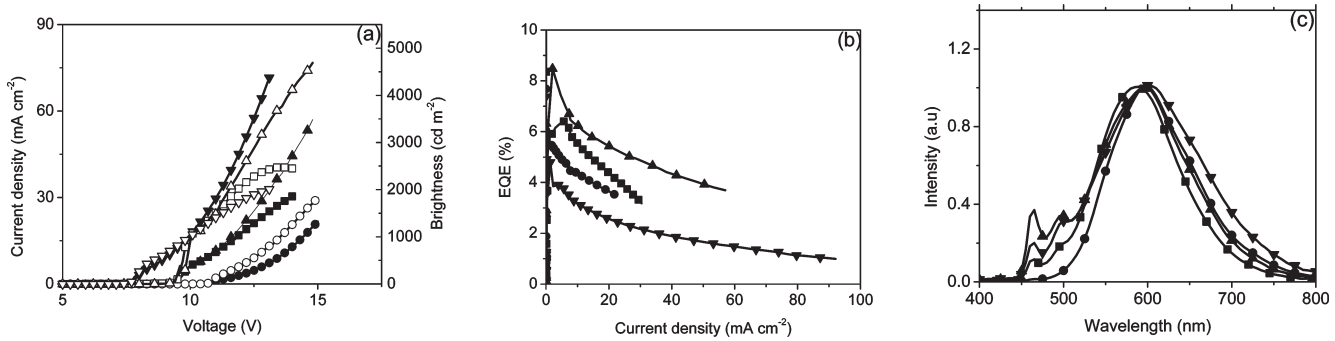

Figure 3. (a) Graph showing the properties of POSS-macromolecules-based devices: (a) current density (solid symbols) and luminance (open symbols) versus bias voltage characteristics of devices with configurations of ITO/PEDOT:PSS/POSS(FPt-6)$_1$(CBZ)$_7$, POSS(FPt-6)$_2$(CBZ)$_6$, and POSS(FPt-6)$_1$(O-mCP)$_7$ + 30% OXD-7/TPBI/CsF/Al. (b) Graph showing the external quantum efficiency-current density properties; (c) Graph showing the normalized EL spectra. [Throughout the figure, data for ITO/PEDOT:PSS/POSS(FPt-6)$_1$(CBZ)$_7$ are denoted by squares, data for POSS(FPt-6)$_2$(CBZ)$_6$ are denoted by circles, and data for POSS(FPt-6)$_1$(O-mCP)$_7$) + 30% OXD-7/TPBI/CsF/Al are denoted by upward-pointing triangles. Downward-pointing triangles denotes data for the control (ITO/PEDOT:PSS/PVK + 30% OXD-7 + 12% FPt/TPBI/CsF/Al) devices.]

Table 2. Summary of Device Characteristics Taken at a Forward Light Output of ~500 cd m^{-2}

	Value @ 500 cd m^{-2}					
device	driving voltage, Bias [V]	current density, J [mA/cm^2]	external quantum efficiency, EQE [%]	power efficiency, PE [lm/W]	luminous efficiency, LE [cd/A]	CIE[a]
ITO/PEDOT:PSS/POSS(FPt-6)$_1$(O-mCP)$_7$ + OXD-7/CsF/Al	8.5	5.94	3.9	3.1	8.5	0.46, 0.44
ITO/PEDOT:PSS/POSS(FPt-6)$_1$(O-mCP)$_7$ + OXD-7/ TPBI/CsF/Al	9.7	3.35	7.9	5.7	17.7	0.46, 0.44
ITO/PEDOT:PSS/PVK + OXD-7 + FPt/TPBI/CsF/Al	8.5	6.16	3.6	2.9	7.8	0.48, 0.45
ITO/PEDOT:PSS/POSS(FPt-6)$_1$(CBZ)$_7$ + OXD-7/TPBI/CsF/Al	9.8	3.66	6.6	5.4	16.8	0.48, 0.48
ITO/PEDOT:PSS/POSS(FPt-6)$_2$(CBZ)$_6$ + OXD-7/TPBI/CsF/Al	12.3	4.07	5.1	3.1	12.0	0.53, 0.46

[a] Commission International de'l'Éclairage (CIE) coordinates.

play an important role in carrier transport. The turn-on voltage of POSS(FPt-6)$_1$(O-mCP)$_7$ devices is ca. 8.2 V. A voltage of 9.7 V is required to achieve 500 cd m^{-2}, which is ca. 1.2 V higher than that of the control PVK devices.

All POSS-based devices show higher EQE values than the reference PVK device (see Figure 3b). The EQE value increases as the FPt-6 moiety content on the POSS macromolecules decreases. In particular, the POSS(FPt-6)$_1$(O-mCP)$_7$ device shows a peak EQE value of 8.4% and luminance efficiency of 18.9 cd A^{-1}. At a luminance of 500 cd m^{-2}, the EQE, luminance efficiency, and power efficiency values are 7.9%, 17.7 cd A^{-1}, and 5.7 lm W^{-1}, respectively. These values are ca. 2 times higher than those of the control PVK device (3.6%, 7.8 cd A^{-1}, and 2.9 lm W^{-1}), which is a step forward in enhancing the device efficiency of solution-processable phosphorescent excimer devices.[7] Improved device efficiency in POSS-based devices may be associated with reduced aggregation of FPt molecules and decreased concentration quenching, which have been generally observed among blend-type devices.[11d] This speculation is supported by a comparison of EL spectra. Concentration quenching also accounts for the reduction in device efficiency with increasing amounts of FPt-6 moieties on the POSS materials.

EL spectra of devices are shown in Figure 3c. Compared to the photoluminescence spectra of POSS macromolecules

in the solid state (Figure 1), a decrease in the monomer to excimer/aggregate emission intensity is observed, indicating that excimer/aggregate states may work as hole traps and direct carrier recombination centers in EL process.[6a] The ratio of monomer to excimer/aggregate emission intensity decreases with increased amounts of FPt-6 moieties in POSS macromolecules, leading to variation in the CIE coordinates from (0.46, 0.44) to (0.48, 0.48) to (0.53, 0.46), for the POSS(FPt-6)$_1$(O-mCP)$_7$, POSS(FPt-6)$_1$(CBZ)$_7$, and POSS-(FPt-6)$_2$(CBZ)$_6$ devices, respectively. The EL spectra of the devices are almost independent of drive voltage. IN contrast, the control PVK devices, for which the molar ratio of carbazole to FPt units is higher than that of POSS(FPt-6)$_1$(O-mCP)$_7$ devices, exhibit less monomer emission intensity, which clearly suggests aggregation of the FPt molecules in blend-type devices. The inhomogeneous distribution of FPt molecules in a blend disturbs the energy/charge transfer from the host, and it results in self-quenching, which leads to a reduction in device efficiency.

Conclusions

To conclude, we have reported on the synthesis, photophysics, and electrochemical characterization of FPt-6 and carbazole moieties dual-functionalized POSS macromolecules. Light-emitting devices based on these POSS macromolecules have shown a significant enhancement in EQE, compared to analogous devices having a blend of Pt-complex and polymer matrix. Device efficiency, as well as the ratio of monomer and excimer/aggregate emission intensity in the EL spectra, increases as the FPt-6 moiety content on the POSS macromolecules decreases, which can be attributed to reduced interactions among FPt-6 units and diminished concentration quenching. Our results represent a noticeable improvement in the efficiency of solution-processable phosphorescent excimer devices.

Acknowledgment. G.E.J. acknowledges the FiDiPro program and the Graduate School of Modern Optics and Photonics, Finland. We would like to thank Nitto Denko Technical Corporation for their financial support.